Supporting Information

Unusual Electronic Transport in (1-x)Cu_2Se-(x)$CuInSe_2$ Hierarchical Composites

Yixuan Chen[1,2], Yinying Zhang[3], Ruiming Lu[1], Trevor P. Bailey[3], Ctirad Uher[3], Pierre F. P. Poudeu[1,2,*]

1) *Laboratory for Emerging Energy and Electronic Materials (LE³M), Department of Materials Science and Engineering, University of Michigan, Ann Arbor, MI, 48109, USA.*
2) *Department of Chemical Engineering, University of Michigan, Ann Arbor, MI, 48109, USA.*
3) *Department of Physics, University of Michigan, Ann Arbor, MI, 48109, USA*

**Corresponding Author*: Pierre Ferdinand Poudeu Poudeu

E-mail: ppoudeup@umich.edu; Fax: +1-734-763-4788

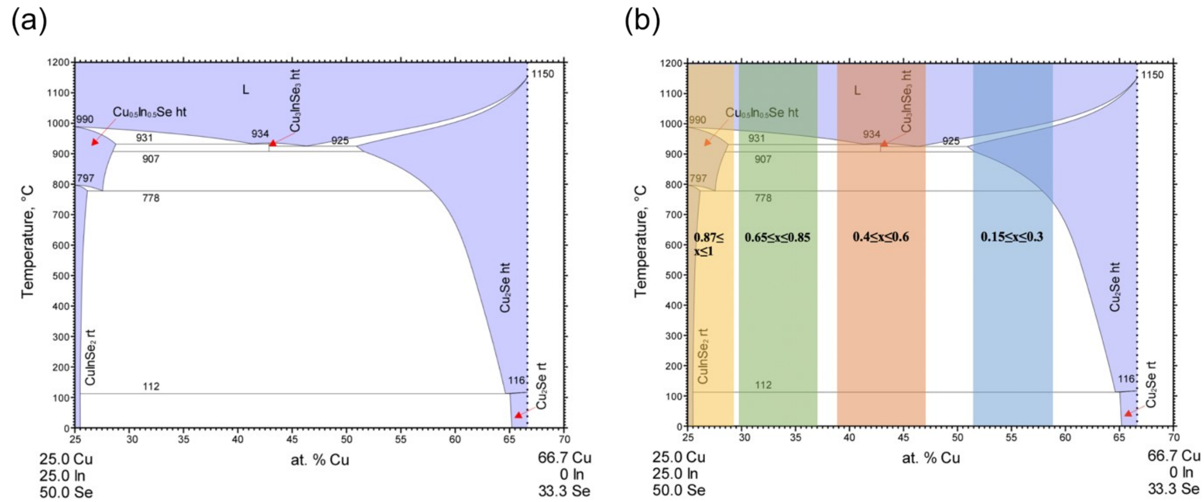

Fig. S1 (a) Phase diagram of Cu_2Se and $CuInSe_2$. (b) The phase diagram is overlaid with stripes representing (1-*x*)Cu_2Se/(*x*)$CuInSe_2$ composites with different *x* values.

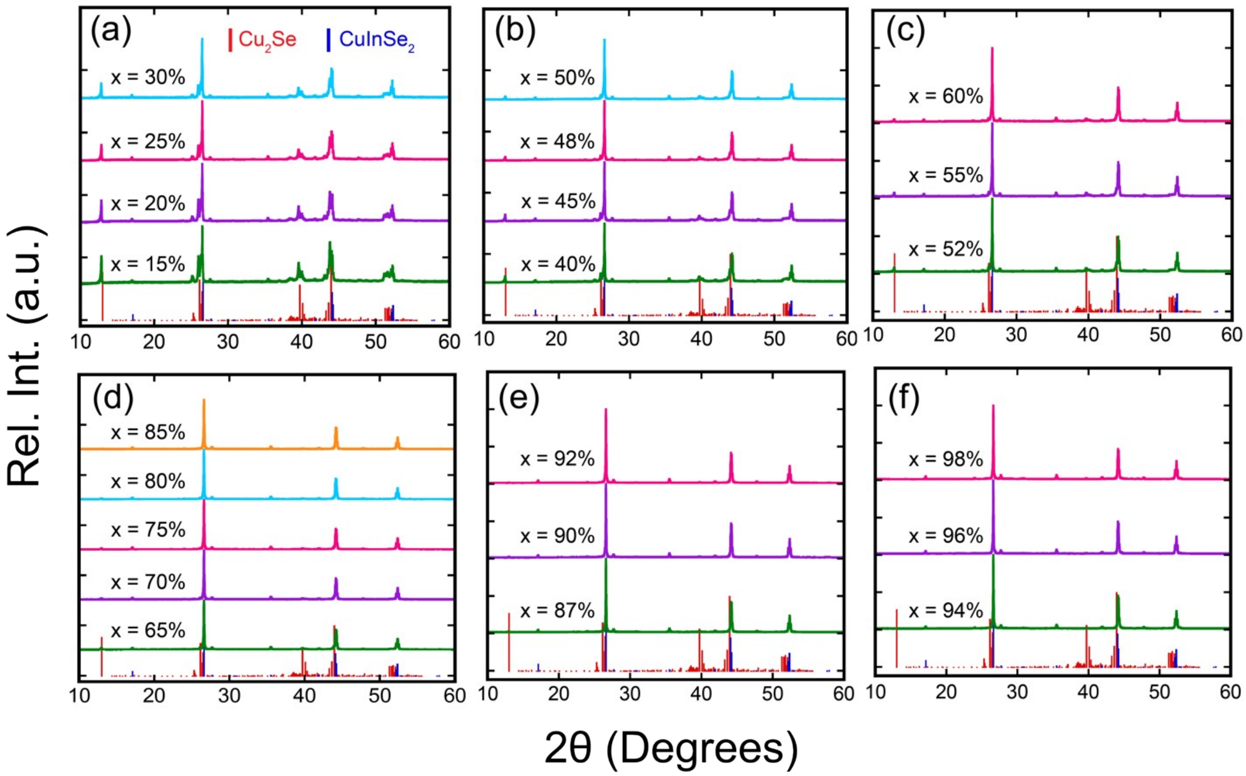

Fig. S2 Powder X-ray diffraction (PXRD) patterns for all as-prepared (1-*x*)Cu_2Se/(*x*)$CuInSe_2$ composites. All diffraction peaks can be indexed with Cu_2Se and $CuInSe_2$ showing high purity of the synthesized composites. The peaks for Cu_2Se quickly diminish since x = 50% (b) and completely disappear at x = 85% (d).

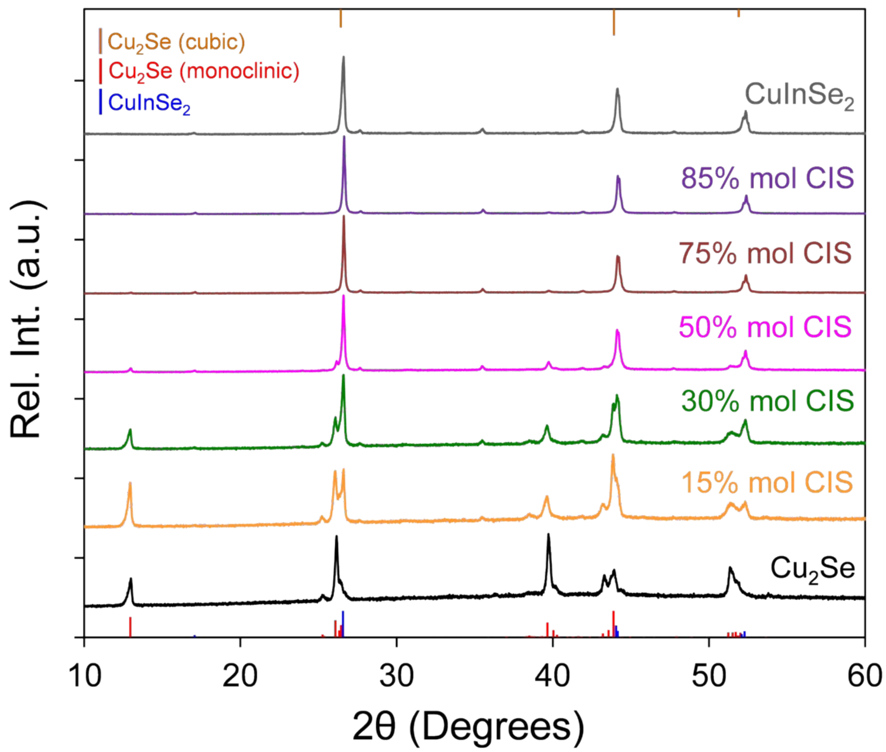

Fig. S3 Representative X-ray diffraction patterns of hot-pressed (1-x)Cu_2Se/(x)$CuInSe_2$ composites. No new phase is observed indicating high purity and good stability of the composites after hot press.

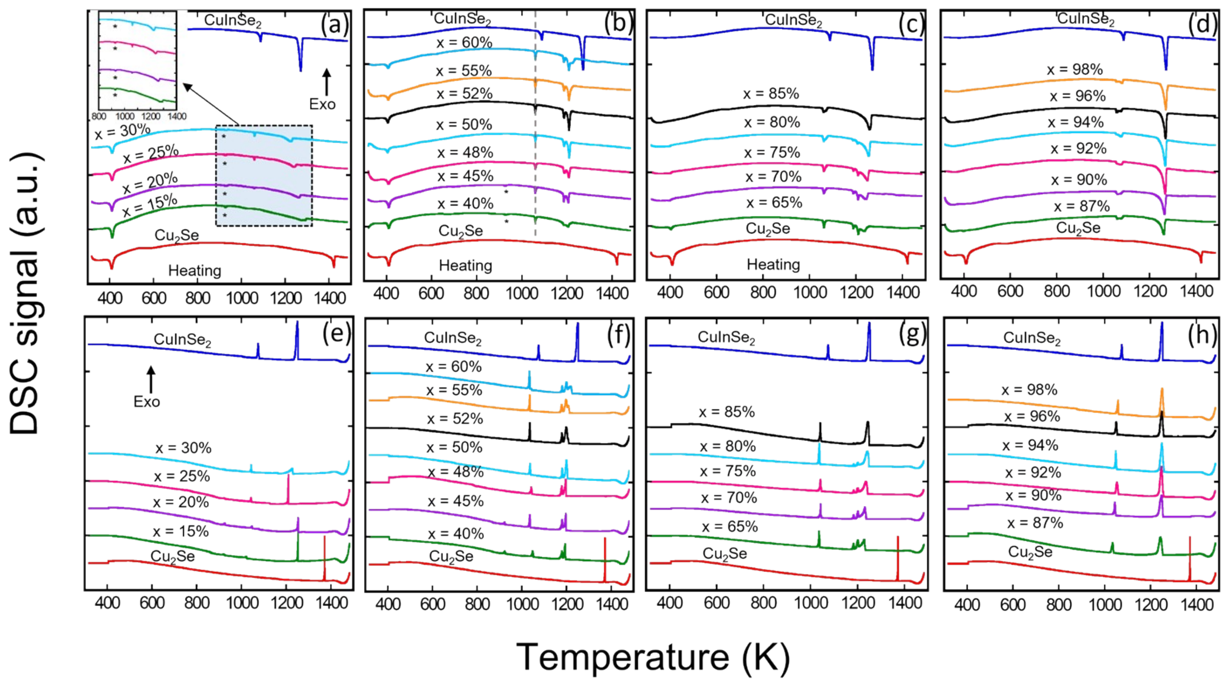

Fig. S4 Differential scanning calorimetry (DSC) curves for all composites. (a) – (d) The major peaks on the heating curves of all composites match well with the phase diagram. The exceptional endothermic peak at ~ 929 K is denoted by *, which suggests the existence of nanoscale $CuInSe_2$ phase. The dashed line is a guide to the eye, showing the small difference between the micron scale phase transition peak of composites and that of bulk $CuInSe_2$. The extinction of phase transition peak for Cu_2Se from $x = 85\%$ also indicates it crystalizes in nanoscale. (e) – (h) Cooling curves for each sample correspond well with the heating curves with a small supercooling effect. The red and blue curves on all graphs are pure Cu_2Se and $CuInSe_2$ synthesized for comparison.

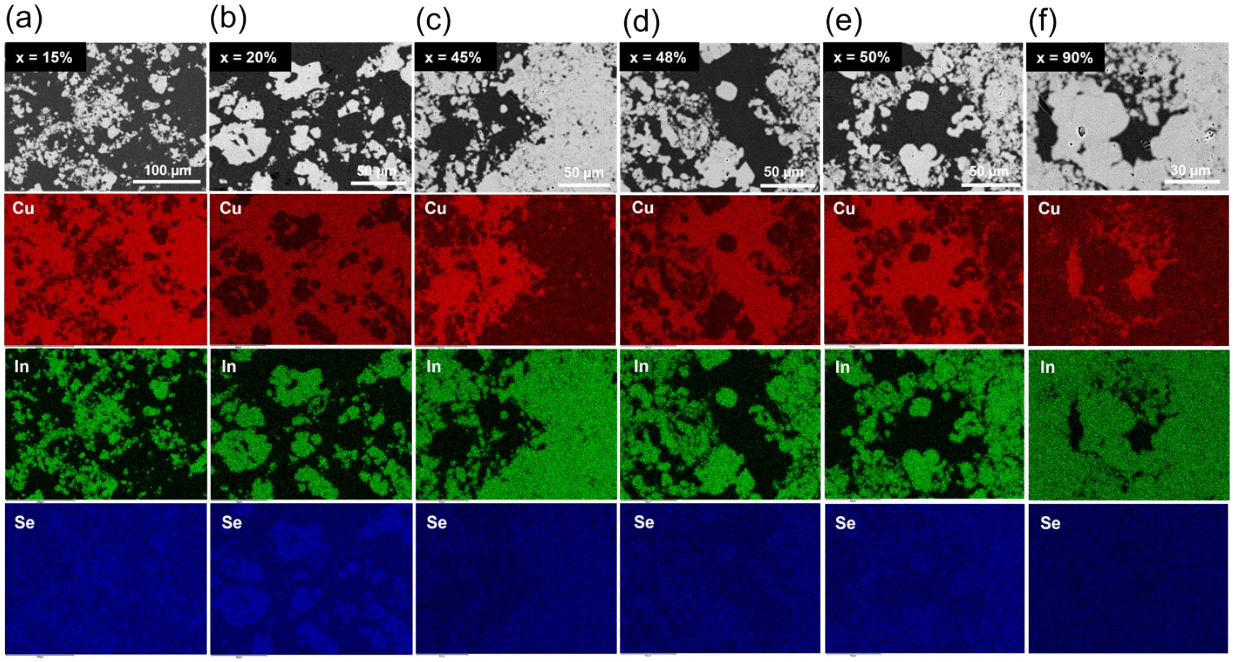

Fig. S5 EDS mapping of selected (1-x)Cu_2Se/(x)$CuInSe_2$ composites. (a) x = 15%; (b) x = 20%; (c) x = 45%; (d) x = 48%; (e) x = 50%; (f) x = 90%. The location and relative size of the $CuInSe_2$ particles in various sample can be clearly tracked following the distribution of In (green) and Se (blue) elements. Likewise, the Cu_2Se phase is also distinguishable following the distribution of Cu (red) element.

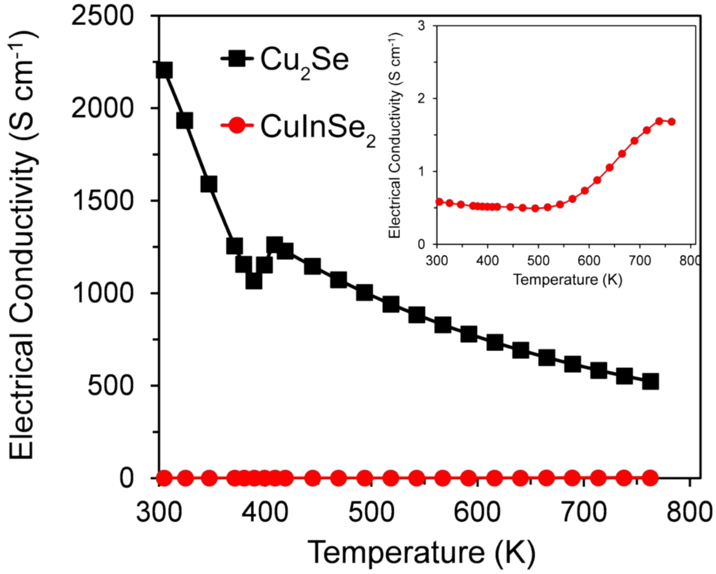

Fig. S6 Temperature-dependent electrical conductivity of Cu_2Se and $CuInSe_2$. Cu_2Se behaves like a heavily doped degenerate semiconductor, while $CuInSe_2$ generally shows the characteristic of an intrinsic semiconductor.

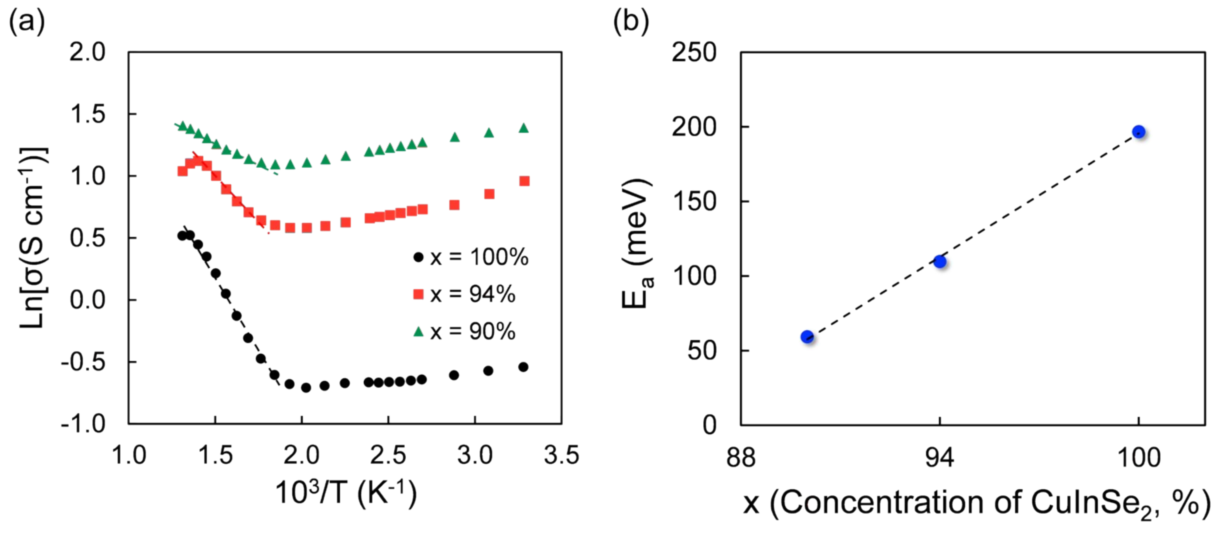

Fig. S7 (a) Arrhenius plot of ln(σ) versus $10^3/T$, giving linear slopes which are used to obtain activation energy of carriers. (b) Variation of the activation energy with the content of $CuInSe_2$, showing a liner decrease with added Cu_2Se.

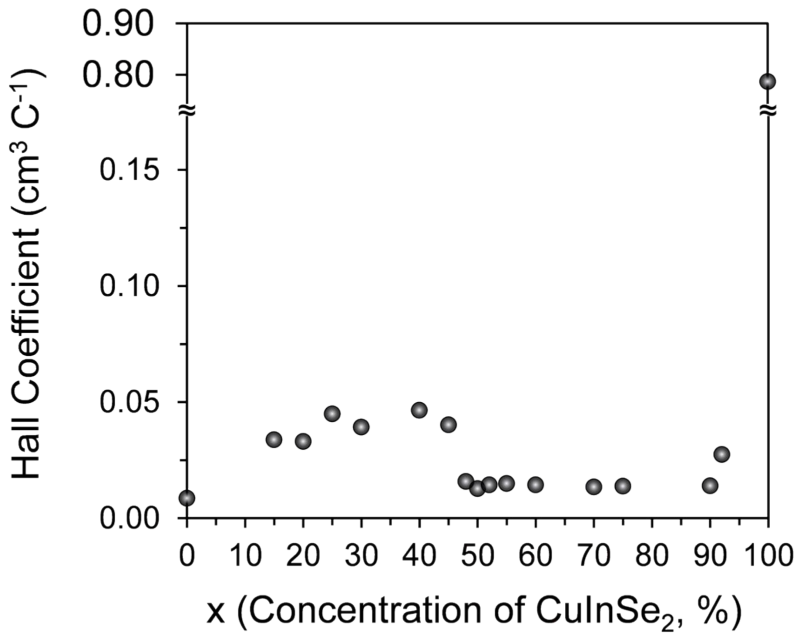

Fig. S8 Measured Hall coefficient of selective samples at 300 K. All samples show positive Hall coefficients, indicating that free holes are the dominant carriers in the composites.

Sample	Cu_2Se phase			$CuInSe_2$ phase		
	Cu (At%)	Se (At%)	In (At%)	Cu (At%)	Se (At%)	In (At%)
0.85CS/0.15CIS	66.45	33.48	0.05	28.05	47.93	23.98
0.52CS/0.48CIS	65.44	34.38	0.17	26.37	49.65	23.98
0.50CS/0.50CIS	65.71	34.23	0.03	26.58	49.51	23.91
0.10CS/0.90CIS	63.45	36.55	0	25.48	50.32	24.18

Table S1 Atomic concentration of each element in both phases of (1-x)Cu_2Se/(x)$CuInSe_2$ composites, determined by EDS point analysis. For each value, at least 10 different points in distinct regions were collected and averaged.